

TABLE III: Molar Fraction F_b of Bound Water and the NMR Relaxation Parameters (Calculated As Explained in the Text)^a

temp, °C	T_2 , ms			F_b	B_w , g of water/g of DNA
	obs	bound	free		
0	72.3	30.51	2685	0.42	0.37
25	152.7	48.41	4806	0.31	0.28

^a $T_2(\text{obs})$: observed NMR relaxation time. $T_2(\text{bound})$: calculated value for bound water using τ_{db} . $T_2(\text{free})$: calculated value for free water using τ_{df} . F_b : molar fraction of bound water. B_w : the relative amount of bound water.

interaction between two nearest protons prevails in the free water. Therefore, the rotational correlation time stands for the correlation time of the dipole-dipole interaction of free water.

If we use $r = 1.51 \times 10^{-8} \text{ cm}^{11,12}$ for the interproton distance in H_2O , we calculate the rotational correlation times τ_c listed in Table II. The values of τ_c obtained from eq 4 using the experimental value of T_2 and the dielectric relaxation times obtained from the TDR measurements are given in Table II.

Since the rotational correlation time is theoretically related to the dielectric relaxation time:¹¹

$$\tau_c = \tau_d/3 \quad (6)$$

we can compare the τ_c values obtained from the NMR with that obtained from the TDR. As shown in Table II, this value τ_c is between the $\tau_d/3$ values for bound and free water. This suggests that fast exchange between bound and free water takes place on the NMR time scale. In this case, the NMR relaxation time T_2 is described as follows:⁴

$$\frac{1}{T_2} = \frac{F_b}{T_{2b}} + \frac{1 - F_b}{T_{2f}} \quad (7)$$

where T_2 is the observed relaxation time, T_{2b} and T_{2f} are NMR relaxation times of bound and free water, respectively, and F_b is the molar fraction of bound water.

The relaxation times T_{2b} and T_{2f} can be calculated by substituting the $\tau_d/3$ values in Table II into τ_c in eq 4. Thus, the molar fraction of bound water is calculated from eq 7 and are given in Table III. Our results are comparable to the solvation sphere required to maintain the B form of DNA in solution.^{2,5}

Our results demonstrate that the exchange between bound and free water in the DNA solution takes place as fast as experimental NMR time scales, and therefore the observed relaxation time T_2 is a weighted average. On the other hand, the rate of this process is slow on the TDR time scale, and therefore separate measurements associated with bound and free water are possible.

References and Notes

- (1) Kuntz, I. D., Jr.; Kauzman, W. *Adv. Protein Chem.* **1974**, *28*, 239.
- (2) Umehara, T.; Kuwabara, S.; Mashimo, S.; Yagihara, S. *Biopolymers* **1990**, *30*, 649.
- (3) Mashimo, S.; Ota, T.; Shinyashiki, N.; Tanaka, S.; Yagihara, S. *Macromolecules* **1989**, *22*, 1285.
- (4) Woessner, D. E.; Zimmerman, J. R. *J. Phys. Chem.* **1963**, *67*, 1590.
- (5) Mashimo, S.; Umehara, T.; Kuwabara, S.; Yagihara, S. *J. Phys. Chem.* **1989**, *93*, 4963.
- (6) Farrar, T. C.; Becker, E. D. *Pulse and Fourier Transform NMR*; Academic Press: New York, 1971; Chapters 2 and 4.
- (7) Mashimo, S.; Umehara, T.; Ota, T.; Kuwabara, S.; Shinyashiki, N.; Yagihara, S. *J. Mol. Liq.* **1987**, *36*, 135.
- (8) Cole, K. S.; Cole, R. H. *J. Chem. Phys.* **1941**, *9*, 341.
- (9) Davidson, D. W.; Cole, R. H. *J. Chem. Phys.* **1951**, *19*, 1484.
- (10) Lynch, L. J. *Magnetic Resonance in Biology*; Cohen, J. S., Ed.; John Wiley & Sons: New York, 1983; Vol. 2, Chapter 5.
- (11) Blinc, A.; Lahjnar, G.; Blinc, R.; Zidansek, A.; Sepe, A. *Magn. Reson. Med.* **1990**, *14*, 105.
- (12) Bloembergen, N. *Nuclear Magnetic Relaxation*; W. A. Benjamin: New York, 1961; Chapter 4.

Controlled Nanofabrication of Highly Oriented Pyrolytic Graphite with the Scanning Tunneling Microscope

Robin L. McCarley,[†] Samuel A. Hendricks, and Allen J. Bard*

Department of Chemistry and Biochemistry, The University of Texas at Austin, Austin, Texas 78712
(Received: July 13, 1992; In Final Form: October 8, 1992)

The formation and selective etching of recessed features of various shapes in highly oriented pyrolytic graphite (HOPG) in air were accomplished by use of the scanning tunneling microscope with positive substrate bias voltages of +1500 to +3000 mV and tunneling currents of less than 2 nA. Etching of the surface was restricted to the scan area and only occurred with positive biases, which suggests that etching occurs by an electrochemical mode of oxidation of the graphite under the tip. Lines with widths as small as 10 nm and squares $25 \times 25 \text{ nm}$ could be formed with monolayer depth (0.34 nm) in the HOPG by varying the time that the tip was rastered over a designated area.

Introduction

We describe here a highly controlled method for the fabrication of nanometer size structures on highly oriented pyrolytic graphite (HOPG) using the scanning tunneling microscope (STM).¹ Recessed lines, squares, and disks could be formed on the basal plane of HOPG by using the STM to etch the surface. Bias voltages (V_b) of +2800 mV (substrate vs tip) with tunneling currents (i_t) of 0.06–2 nA caused layer-by-layer removal of the carbon atoms directly under the tip. Selective etching of existing defects (exposed edge-plane graphite) occurred at bias potentials greater than or equal to +1500 mV. The rate of etching depended upon the magnitude of the bias but was controlled best with +1500

$\text{mV} \leq V_b \leq +2400 \text{ mV}$. Negative substrate biases of the same magnitude did not cause etching of the HOPG. Low biases (50–500 mV) and high tunneling currents (1–4 nA), which bring the tip closer to the HOPG, did not cause removal of material, indicating that etching is not due to physical interaction of the tip with the HOPG. These results suggest that the etching process is probably electrochemical in nature.

The advent of the STM has led to many advances in the characterization of conducting and semiconducting surfaces. There have also been several applications to "nanofabrication" of surfaces.² Such studies are motivated by a desire to understand different approaches to the controlled modification of surfaces at the atomic level with ultimate applications to devices or structures like masks for X-ray lithography. In these the tip voltage is usually pulsed to higher bias voltages to remove or place

[†] Present address: Department of Chemistry, Louisiana State University, Baton Rouge, LA 70803.

material on the substrate of interest. Modification of the surface of HOPG in the presence of water or water vapor by voltage pulses has been demonstrated by several groups and has been attributed to an electron-induced or enhanced ion etching.³⁻⁶ Usually, monolayer deep pits of 4–5-nm diameter were produced. These pits were quite stable under normal STM imaging conditions ($i_t = 0.1$ – 1 nA, $V_b = 10$ – 500 mV). Pits have been reported to form with either positive or negative bias pulses, although the reproducibility using a negative bias pulse was poorer.⁶ More extended structures have been produced by this method by making arrays of holes in the HOPG surface with the most elaborate being an English phrase consisting of four words.²

We show here that complex structures can be written into HOPG in air by controlling the bias potential, tunneling current, and tip raster area during scanning in a systematic manner. For example, use of $i_t = 0.25$ nA and $V_b = +2800$ mV allowed us to fabricate monolayer-deep lines with widths of 10 nm as well as squares with dimensions from 25×25 nm to 300×300 nm. These features, as well as pits formed by thermal treatment⁷ or voltage pulsing,³⁻⁶ can be enlarged (without damaging the rest of the basal plane around the feature) by scanning the feature area with biases of 1500–2400 mV. Only the edge-plane sites are reactive enough to be removed in this potential range. Lower biases (50–500 mV) with high tunneling currents (1–4 nA) did not cause etching, which indicates that etching occurred by a chemical reaction rather than by abrasion of the surface by the tip. We believe that the etching is due to an electrochemical oxidation of the graphite directly under the tip in a layer of adsorbed water. Previous reports of pits formed by potential pulsing have shown that water is necessary for successful pit formation.³⁻⁶ Adsorbed water allows localized oxidation of graphite at the HOPG surface under the tip and reduction of water at the tip within the very thin layer (approximately 0.5 nm thick) of water on the surface.⁸

Experimental Section

Instrumentation. Images were obtained with a NanoScope II scanning tunneling microscope (Digital Instruments, Santa Barbara, CA) using mechanically cut (GC Electronics diagonal cutters) Pt/Ir (80:20) wire or electrochemically etched (10 V ac in 1 M KOH) tungsten wire. Images were obtained in the topographic mode (constant current) with $V_b = 50$ – 500 mV and $i_t = 0.25$ nA. If necessary, images were slightly filtered using the low pass filter option of the NanoScope II software.

Chemicals. All chemicals were reagent grade or better. Highly oriented pyrolytic graphite (a generous gift from A. Moore at Union Carbide, Parma, OH) was freshly cleaved before each experiment.

Results and Discussion

Pit Formation with Potential Pulses. Several groups have noted the reproducible formation of pits in HOPG by pulsing the potential of the substrate positive (with respect to the tip) in humid environments or in water.³⁻⁶ Use of negative potential pulses was also reported to give qualitatively similar results.⁶ We were not successful, however, at producing reproducible pits with negative pulses with either Pt/Ir or W tips and observed the following. Negative pulses with Pt/Ir tips always tended to deposit material onto the HOPG, presumably from oxidation and removal of material from the tip. Usually the tip was so heavily damaged and image quality so poor after a negative pulse that a new tip had to be used. When we used electrochemically-etched W tips in the negative potential pulse mode, the HOPG surface was damaged by what appeared to be either the tip touching the surface or material being deposited from the tip. Here, application of a negative pulse probably caused the tip to be oxidized and material to be transferred to the HOPG surface.⁹ With a W tip, oxide formation at higher potentials would cause it to become insulating and to make physical contact with the surface and damage the HOPG. We provide further evidence for this in the section below concerning etching of the HOPG. Penner et al.⁶ used only W tips and did not show images of the HOPG surface

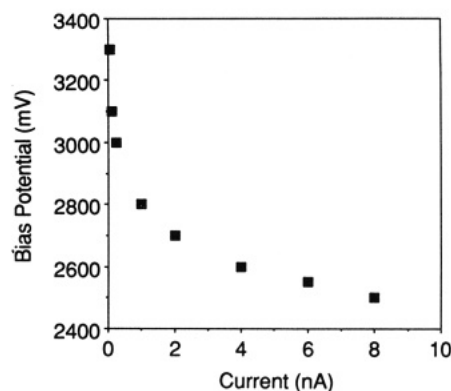


Figure 1. Plot of pit initiation bias for 8-nm-diameter pits versus initial tunneling current.

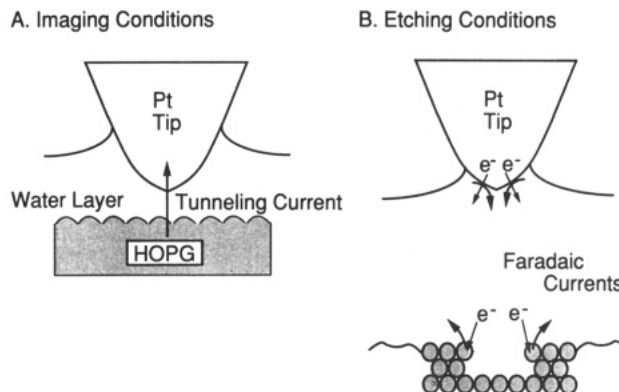


Figure 2. Schematic of conditions for imaging versus etching. Probable reactions during etching are (tip) $2\text{H}_2\text{O} + 2e^- \rightarrow \text{H}_2 + 2\text{OH}^-$ and (substrate) $\text{C} + n\text{H}_2\text{O} \rightarrow \text{CO}_n + 2n\text{H}^+ + 2ne^-$ ($n = 1$ or 2).

using negative pulses, although they reported qualitatively similar behavior for both positive and negative pulses. In our experiments, we have not been able to form reproducible pits on HOPG using negative potential pulses.

Pits could be formed on HOPG using either Pt/Ir or W tips and positive potential pulses. The smallest pit we were able to make had a diameter of approximately 4 nm. Larger pits could be formed by increasing the magnitude or duration of the voltage pulse. To study the dependence of threshold potential for pit formation on the tip-to-sample distance, we performed a series of experiments (using Pt/Ir tips) where the tunneling current was varied and the potential required for reproducible formation of a 8-nm pit was recorded. The results show that the curve approaches a minimum value of approximately 2300 mV at larger tunneling currents (Figure 1). We propose that this represents the overall potential for the oxidation of graphite and reduction of water at a Pt surface.¹⁰ The hydroxyl radical is probably not involved in the formation of pits by potential pulsing, because the potential of such a reaction would be greater than the potential for the oxidation of graphite.¹¹ Moreover, with HOPG that had been exposed to dilute acid solutions (1 M HClO_4), rinsed with water, and dried, pits could be produced at lower potentials (approximately 100 mV less at a given i_t) than for untreated HOPG. Deionized water blanks showed no difference. This indicates that the presence of hydrogen ion (which is more easily reduced than water at the tip) caused a decrease in the potential of the overall process. We cannot delineate the details of the pit formation mechanism, but from the above data and that which follows, we conclude that the pit formation is due to an electrochemical process, as depicted in Figure 2B.

Etching of Defects in HOPG. Figure 3 ($t = 0$) is an STM image of a 4-nm-diameter, two-monolayer-deep pit formed by applying a +3000-mV pulse with $i_t = 0.25$ nA for approximately 0.5 s. The pit was then imaged at $V_b = +1500$ mV and $i_t = 0.25$ nA for different lengths of time. As can be seen in Figure 3, the pit grew outward with scanning time. The later images clearly show that

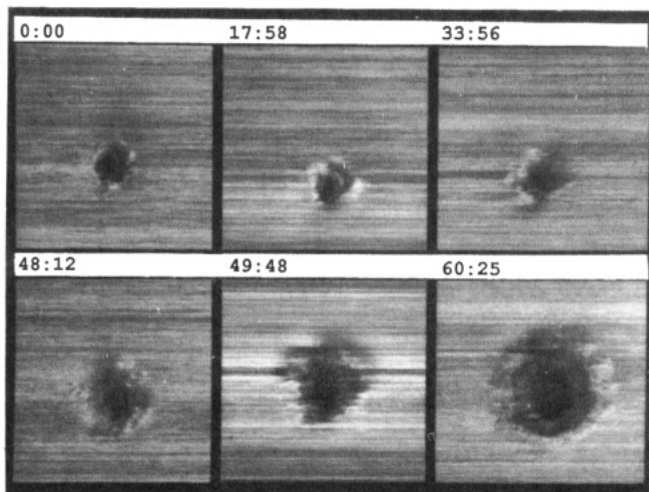


Figure 3. The 50×50 nm constant-current STM images of a two-monolayer-deep pit formed with a +3000-mV pulse with $i_t = 0.25$ nA and then etched with $V_b = +1500$ mV and $i_t = 0.25$ nA as a function of time in minutes. Z range is 0–5 nm.

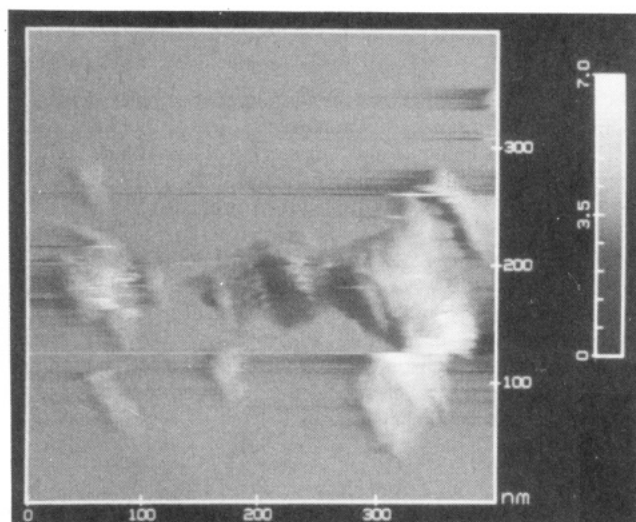


Figure 4. A 400×400 nm constant-current STM image (using a W tip) of an area where a pit was made with a +3000-mV pulse, followed by imaging at $V_b = -1500$ mV, $i_t = 0.25$ nA for 2 min.

the second layer of the pit also etched, but the basal plane in the scanned area was unaffected. Similar experiments with $+1500 \text{ mV} \leq V_b \leq +2400 \text{ mV}$ bias exhibited growth rates which scaled with the bias potential. At $V_b > +2800 \text{ mV}$, the etching was very fast and the basal plane of the scanned area also began to form pits. (At this tunneling current the threshold potential for producing pits by pulsing is approximately +3000 mV.) Higher tunneling currents also increased the etching rate, similar to the effect seen with the voltage pulsing in Figure 1. Low bias voltages and high tunneling currents during imaging, which bring the tip closer to the HOPG (Figure 2A), *did not cause etching*. Use of negative biases of up to -1500 mV with Pt/Ir tips did not cause etching of the defects. Potentials more negative than -1500 mV caused the Pt/Ir tip to become unstable, and material was deposited on the HOPG from the tip. When W tips were used at these high biases, the pit was not etched but rather torn open; the pit edges were peeled outward from the sides (see Figure 4). Such negative bias results were reproducible for various-sized pits. At such positive tip potentials (substrate negative) the W probably formed an insulating oxide by an anodic process that made the tip move closer to the HOPG to maintain the same tunneling current; this allowed the tip to make physical contact with the graphite and damage the edges of the pit. There was no damage done to defects, if the tunneling current was $0.25\text{--}8 \text{ nA}$ with bias voltages of -25 to -500 mV (voltages insufficient to drive W tip oxidation). However, HOPG defects could be systematically

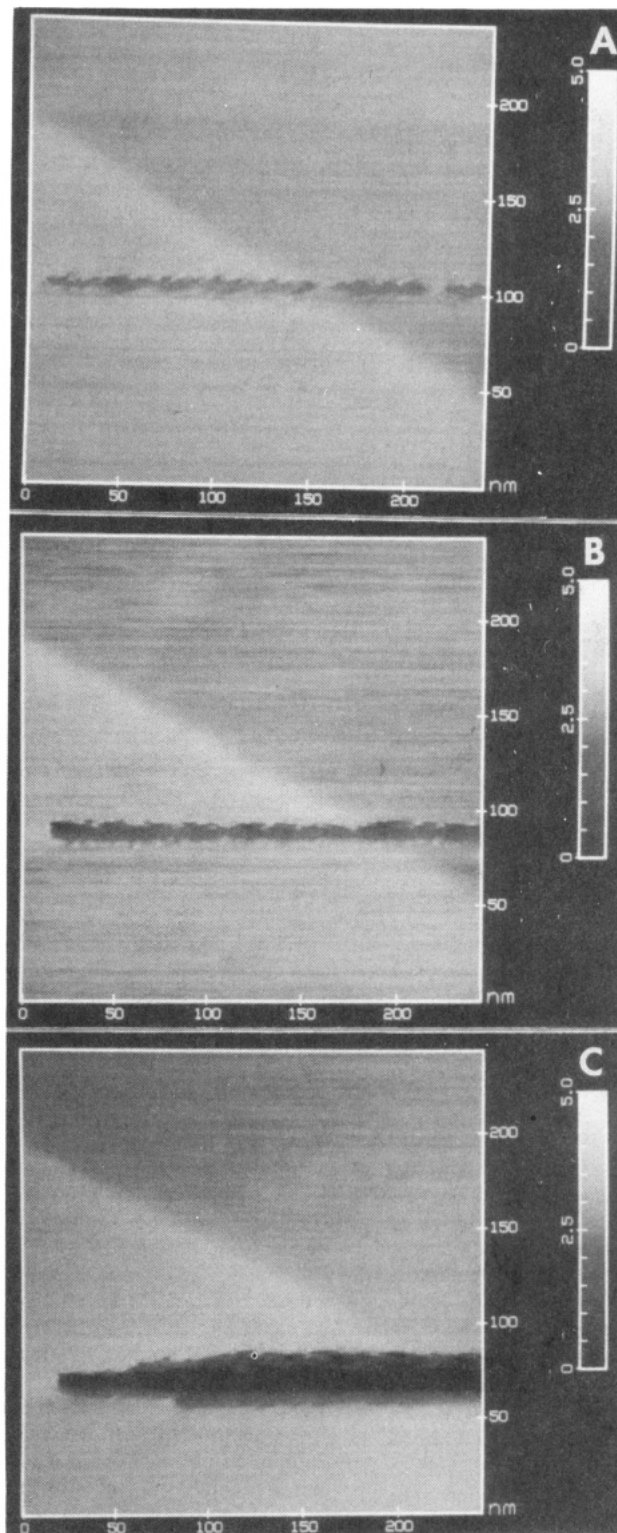


Figure 5. Constant-current STM images of recessed lines formed by disabling the y -piezoelectric drive and scanning the x -piezo at 19 Hz with $V_b = +2800 \text{ mV}$ and $i_t = 0.25 \text{ nA}$ for 10, 30, and 60 s for (A), (B), and (C), respectively. Z range is 0–5 nm.

etched using W tips at high positive substrate biases, under conditions similar to those described for the Pt/Ir tips. Thus, at high negative substrate bias, the tips (Pt/Ir or W) were oxidized, and depending on the type of tip, uncontrolled deposition of tip material or damage of the surface by the tip occurred, which is consistent with an electrochemical process where the tip is oxidized. The results with a positive substrate bias also give support to the electrochemical model (Figure 2B). Under these conditions, the tip is negative and reduction of H_2O or H^+ occurs, while oxidation of HOPG takes place under the tip. These results are similar to

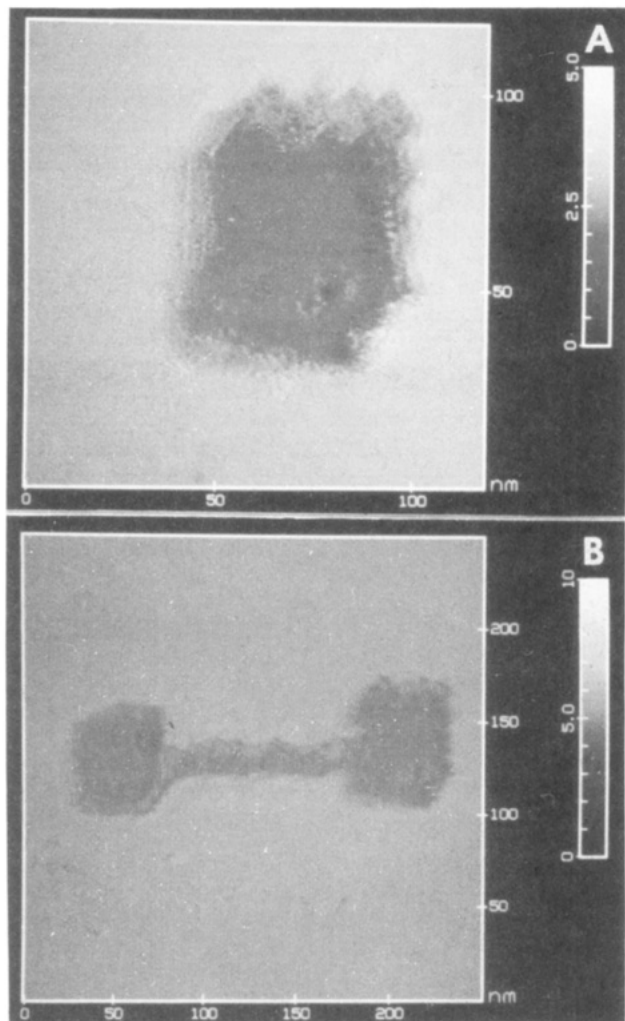


Figure 6. Constant-current STM images of recessed features. (A) 50×50 two-monolayer-deep square. Z range is 0–5 nm. (B) Two 50×50 two-monolayer-deep squares connected with a two-monolayer-deep line. Z range is 0–10 nm.

those we obtained during the deposition of metals and etching of surfaces using the scanning electrochemical microscope (SECM), where the reaction was shown to be localized under the tip.^{12,13} Indeed, under high bias and low current conditions the STM may be operating largely in the SECM mode.

Fabrication of Complex Structures. To test the specificity, range, and resolution of the STM etching of HOPG using high bias voltages, we fabricated various-shaped structures of different dimensions. Figure 5A is a constant-current image of a 10-nm-wide, 0.34-nm-deep line drawn in HOPG. This monolayer-deep line was made by disabling the *y*-piezoelectric drive and scanning the *x*-piezo at 19 Hz with $V_b = +2800$ mV and $i_t = 0.25$ nA for 10 s. Increasing the exposure time to 30 and 60 s produced the lines shown in Figure 5, B and C. The depth of the 30-s line is 0.78 nm (two monolayers), and its width is only slightly larger than the 10-s line (13.2 nm vs 10 nm). Line width increased to 45 nm and depth to 3.4 nm for the 60-s exposure time. This width increase was probably due to etching from the sides of the tip as the tip went deeper to maintain the required current at the recessed surface. We could reproducibly produce lines in HOPG of various

depths and widths with tips which gave clean images (no double-tip effects). The narrowest, continuous line fabricated had a 10-nm width (Figure 5A). Scanning the *x*-piezo to give longer lines did not seem to affect the quality of the lines, and we have drawn lines up to $0.75 \mu\text{m}$ long with no loss in width or depth resolution.

Other shapes such as rectangles or squares could be produced by scanning over one or multiple areas. Figure 6A is a two-monolayer-deep 50×50 nm square formed in HOPG by scanning a 50×50 nm area at 26 Hz for approximately 30 s at $V_b = +2800$ mV and $i_t = 0.25$ nA followed by an "edge cleaning" etch at $V_b = +2000$ mV and $i_t = 0.25$ nA for approximately 3 min. The purpose of the lower bias etch after the pit was formed was to decrease the jagged nature of the approximately square pit. Rectangles could be made by moving the scan area to an edge with $V_b = +1500$ to $+2400$ mV to selectively etch the pit edge. This defect etching mode often exposed smaller defects in the lower HOPG layers, as shown in Figure 6A. These smaller pits are due to the initially high bias etching. More complex structures can be made by using this etching technique. In Figure 6B two pits were formed as previously described, and then a two-monolayer-deep line was drawn to connect them by using the conditions from Figure 5B. Structures such as these can be routinely fabricated next to others without damage to the existing features; pits and lines could be made as close as 10 nm to each other.

Conclusion

We have demonstrated that the formation of complex, recessed features on HOPG is readily achieved by use of the STM with high bias voltages in humid air. The etching of basal-plane HOPG occurred when the substrate bias was raised above $+2600$ to $+2800$ mV with $i_t = 0.25$ – 2 nA. Controlled etching of edge-plane HOPG was found to take place with biases of $+1500$ to $+2400$ mV and tunneling currents of 0.25 – 2 nA. Etching did not take place when negative substrate biases were used. We conclude that the etching occurs in the SECM mode by electrochemical oxidation of the graphite under the tip in a thin, adsorbed layer of water. Both the threshold potential for etching and the sign of the etching potential indicate that an electrochemical reaction caused removal of carbon atoms from the surface.

Acknowledgment. Support of this work by the Office of Naval Research is gratefully acknowledged. R.L.M. acknowledges the National Science Foundation for a Postdoctoral Fellowship received in 1991 (CHE-9101924).

References and Notes

- (1) Binnig, G.; Rohrer, H. *IBM J. Res. Dev.* **1986**, *30*, 355.
- (2) Quate, C. F. In *Scanning Tunneling Microscopy and Related Methods*; Rohrer, H., Behm, R. J., Garcia, N., Eds.; Kluwer: Dordrecht, 1990.
- (3) Albrecht, T. R.; Dovek, M. M.; Kirk, M. D.; Lang, C. A.; Quate, C. F.; Smith, D. P. E. *Appl. Phys. Lett.* **1989**, *55*, 1727.
- (4) Terashima, K.; Kondoh, M.; Yoshida, T. *J. Vac. Sci. Technol.* **1990**, *A8*, 581.
- (5) Mizutani, W.; Inukai, J.; Ono, M. *Jpn. J. Appl. Phys.* **1990**, *29*, L815.
- (6) Penner, R. M.; Heben, M. J.; Lewis, N. S.; Quate, C. F. *Appl. Phys. Lett.* **1991**, *58*, 1389.
- (7) Chang, H.; Bard, A. J. *J. Am. Chem. Soc.* **1991**, *113*, 5588.
- (8) Mate, C. M.; Erlandsson, R.; McClelland, G. M.; Chiang, S. *Surf. Sci.* **1989**, *208*, 473.
- (9) Kim, Y.-T.; Bard, A. J. *Langmuir* **1992**, *8*, 1096.
- (10) Bard, A. J.; Faulkner, L. R. In *Electrochemical Methods*; Wiley: New York, 1980.
- (11) McCreery, R. L. In *Electroanalytical Chemistry*; Bard, A. J., Ed.; Marcel Dekker: New York, 1991; Vol. 17.
- (12) Husser, O. E.; Craston, D. H.; Bard, A. J. *J. Electrochem. Soc.* **1989**, *136*, 3222.
- (13) Lin, C. W.; Fan, F.-R. F.; Bard, A. J. *J. Electrochem. Soc.* **1987**, *134*, 1038.